Contact Angles for Liquid Drops at a Model Heterogeneous Surface Consisting of Alternating and Parallel Hydrophobic/Hydrophilic Strips

Jaroslaw Drelich,*,† James L. Wilbur,‡ Jan D. Miller,† and George M. Whitesides‡

Department of Metallurgical Engineering, University of Utah, Salt Lake City, Utah 84112, and Department of Chemistry, Harvard University, Cambridge, Massachusetts 02138

Received July 7, 1995. In Final Form: January 2, 1996⊗

Model heterogeneous surfaces consisting of alternating and parallel 2.55 μm hydrophobic and 2.45 μm hydrophilic strips were prepared on a gold film by patterning self-assembled monolayers of hexadecanethiol and mercaptohexadecanoic acid using an elastomer stamp. The advancing and receding contact angles were measured for liquid drops (distilled water, buffer solutions with pH = 8.0, 10.0, and 11.0, ethylene glycol, glycerol, and formamide) placed on this specially prepared surface. Contortion of the three-phase contact line is a significant property of these systems. Both contact angles, advancing and receding, were 2−10° lower when measured with the strips normal to the three-phase contact line than those measured with the strips tangential to the three-phase contact line. For most of the systems examined, experimental contact angles, when measured for the liquid drop edge situated along the strips of the model heterogeneous surface (noncontorted three-phase contact line), were in an agreement with theoretical values calculated from the Cassie equation. Also, for most of the systems examined, there was an agreement of experimental contact angles, as measured for the liquid drop edge located normal to the strips (i.e., when the three-phase contact line was contorted), with theory calculated from the modified Cassie equation, including the line-tension term. Only in selected cases could the theory as expressed by the Cassie equation or the modified Cassie equation not predict the experimental contact angles. These were the systems in which the liquid phase interacted strongly with COOH groups of the self-assembled monolayer and completely spread over this hydrophilic portion of the surface.

Introduction

Over forty years ago, Cassie[1] proposed that the contact angle (θ^C) for a liquid at a composite solid surface can be predicted theoretically from a simple equation incorporating the composition of a solid surface and its wetting characteristics. For a two-component surface this equation is[1]

$$\cos\theta^C = f_1 \cos\theta_1 + f_2 \cos\theta_2 \qquad (1)$$

where f_i is the fractional area of the surface with a contact angle of θ_i and the superscript C designates the contact angle for the heterogeneous surface as proposed by Cassie.

Recent theoretical analysis[2−4] of the free energy for the three-phase system with a heterogeneous solid surface pointed out the limitation of Cassie's approach and indicated that the Cassie equation (eq 1) is not universal but, rather, requires a correction that incorporates the excess free energy associated with the three-phase contact line. This correction is especially recommended for systems with micron-size (a few microns in diameter or less) heterogeneities. On this basis, a new theoretical relationship describing the equilibrium contact angle (θ^{MC}) for a liquid at a heterogeneous surface was derived and proposed.[2−4] For example, if a solid surface is composed of two components, uniformly distributed, the equation describing the contact angle is as follows:[4]

$$\cos\theta^{MC} = f_1 \cos\theta_1 + f_2 \cos\theta_2 - \left(\frac{1}{\gamma_{LV}}\right)\left(\frac{f_1\gamma_{SLV_1}}{r_1} - \frac{f_2\gamma_{SLV_2}}{r_2}\right) \qquad (2)$$

where γ_{LV} is the surface tension for the liquid; r_i is the radius of the three-phase contact line at the i-component of the surface; $\gamma_{SLV_i} = (\delta F_i/\delta L_i)_{T,V,A_{ij},n_i}$ is the line tension; F is the free energy of the system; T, V, A, and L are the temperature, volume, interfacial area, and length of the three-phase contact line, respectively; and the superscript MC designates the modified Cassie contact angle.

The contact angles, θ^C and θ^{MC}, for the model heterogeneous solid surface are distinguished by the drawing presented in Figure 1. In this particular case, the solid surface is composed of alternating and parallel strips differing in surface properties (surface/interfacial tension), for simplicity called hydrophobic and hydrophilic strips. A pure liquid at each surface strip forms an intrinsic contact angle (θ_1 and θ_2 where $0° < \theta_1 < 180°$, $0° < \theta_2 < 180°$, and $\theta_1 > \theta_2$) which satisfies the modified Young's equation[5]

$$\gamma_{SV_i} - \gamma_{SL_i} = \gamma_{LV}\cos\theta_i + \frac{\gamma_{SLV_i}}{r_i} \qquad (3)$$

where γ_{SV} and γ_{SL} are the interfacial tensions for the solid/vapor and solid/liquid interfaces, respectively.

Two extremely different positions of the three-phase contact line at the model heterogeneous surface are illustrated in Figure 1, for the surface strips parallel and normal to the three-phase contact line.

For the first position, the wetting line is smooth because it is situated along a strip. Assuming that the dimensions of the strips are very small—micron-size or less—the

* To whom correspondence should be addressed. E-mail: jdrelich@mines.utah.edu. Phone: (801)581-6814. Fax: (801)581-4937.
† University of Utah.
‡ Harvard University.
⊗ Abstract published in *Advance ACS Abstracts,* March 15, 1996.
(1) Cassie, A. B. D. *Discuss. Faraday Soc.* **1948**, *3*, 11.
(2) Drelich, J.; Miller, J. D. *Part. Sci. Technol.* **1992**, *10*, 1.
(3) Drelich, J. Ph.D. Dissertation, University of Utah, **1993**.
(4) Drelich, J.; Miller, J. D. *Langmuir* **1993**, *9*, 619.
(5) Boruvka, L.; Neumann, A. W. *J. Chem. Phys.* **1977**, *66*, 5464.

0743-7463/96/2412-1913$12.00/0

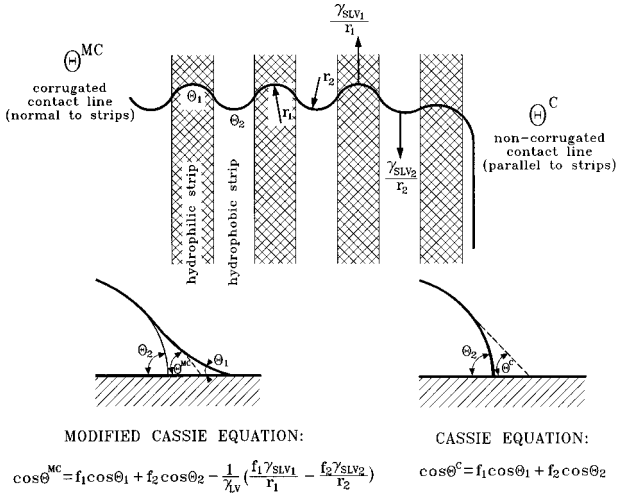

Figure 1. Schematic of a three-phase contact line for a liquid drop at a heterogeneous surface consisting of alternating and parallel hydrophobic and hydrophilic strips. When the three-phase contact line is normal to the strips, the equilibrium contact angle is described by the modified Cassie equation, θ^{MC}. On the other hand, the equilibrium contact angle is predicted by the Cassie equation, θ^{C}, for a three-phase contact line which is situated parallel to the strips. Both equilibrium contact angles, normal and parallel to the strips, are experimentally observed for systems for micron-size strips. The local contact angles at hydrophilic, θ_1, and hydrophobic, θ_2, strips cannot be distinguished during contact angle measurements for such systems using low-magnification goniometers and microscopes, such as commonly used in traditional surface chemistry laboratories. Also, the distortion of the drop base, as affected by the micron-size strips and illustrated in the figure, is difficult to detect with these instruments. The effect of local contact angles, θ_1 and θ_2, on the shape of the liquid drop and local distortions of the drop base will complicate the measurements of both contact angles (normal and parallel to the strips) when the width of the strips exceeds the micron-size range.

contact angle as measured for a liquid with the three-phase contact line parallel to the strips should be equal to the theoretical value predictable by the Cassie equation (eq 1). The analysis of the system becomes more complicated for strips of larger dimension, several microns and more. The total free energy of the system may depend on the position of the three-phase contact line (i.e., at which strip type, hydrophilic or hydrophobic, and at what distance from the boundary between the hydrophobic and hydrophilic strips). Under these circumstances several different contact angles are possible (including the thermodynamic equilibrium contact angle which the Cassie equation predicts), due to metastable configurations of the system.[6,7]

Only one equilibrium contact angle describes the situation for the second location of the wetting line presented in Figure 1, when the micron-size strips are normal to the three-phase contact line, i.e., the wetting line is contorted (of course, ideal hydrophilic and hydrophobic surfaces are considered and no hysteresis in contact angle is allowed for both materials, hydrophilic and hydrophobic). The corresponding contact angle is described by eq 2.

According to eqs 1 and 2, a difference between θ^{MC} and θ^{C} depends on the line tension value, which is believed to be extremely small, 10^{-12} J/m $< \gamma_{SLV} < 10^{-9}-10^{-8}$ J/m,[8] and the dimensions of the local deformations of the contorted three-phase contact line (r_1 and r_2). If the dimensions of the heterogeneous mosaics (strips in the model being considered) are too large, the contribution of the linear free energy to the total free energy of the three-phase system is negligible ($\gamma_{SLV}/r \rightarrow 0$ for $r \rightarrow \infty$), and the modified Cassie equation (eq 2) is reduced to the original Cassie equation (eq 1).[4]

Preparation of well-defined heterogeneous surfaces, especially with micron-size heterogeneities, is required in order to verify the hypothesis that the contact angle for the system with a smooth wetting line differs from that for the system with a contorted three-phase contact line. Patterning of self-assembled monolayers (SAMs) of thiols at a gold surface by contact printing using an elastomer stamp[9,10] was found in our previous studies[11] to be a convenient technique for the preparation of model heterogeneous surfaces. Mosaic patterns of 2.5 μm hydrophobic/3 μm hydrophilic strips, and 3 μm $\times$ 3 μm hydrophilic squares separated by 2.5 μm hydrophobic strips were prepared using this technique, and the wetting characteristics of these surfaces were established by contact angle measurements.[11] It was found that experimental advancing contact angles are in good agreement with theory as calculated from the Cassie equation (eq 1) when the three-phase contact line was smooth, i.e., situated along the strips. On the other hand, when the strips were normal to the drop edge, contortion of the three-phase contact line affected the advancing contact angles significantly, and these contact angles were in close agreement with those calculated with the modified Cassie equation (eq 2).

Also in the present contribution, model organic surfaces with alternating and parallel hydrophobic and hydrophilic strips were prepared at Harvard University by patterning SAMs of thiols on a gold surface using an elastomer stamp. These model surfaces were examined by contact angle measurements at the University of Utah in order to further verify the validity of the theoretical analysis as represented by the Cassie and modified Cassie equations. Mostly, advancing contact angles for the model heterogeneous surfaces were measured in the previous studies.[11] In this current research, measurements of both the advancing and receding contact angles were conducted for the model surface composed of alternating and parallel 2.55 μm hydrophobic and 2.45 μm hydrophilic strips. The experimental data again support our previous statement on the effect of the three-phase contact line contortion on the contact angle for systems with micron-size heterogeneities.

Experimental Procedure

Substrate Preparation. Electron-beam evaporation of gold (Materials Research Co.; 99.999%) onto silicon [100] test wafers (Silicon Sense) at room temperature provided 1000 Å thick gold films. Titanium (Johnson Mathey, 99.99%; ~5−25 Å thick) was used as an adhesion promoter between the gold and the silicon surface.

Formation of Monolayers. Silicon wafers coated with gold were fractured into rectangular slides (1−2 cm × 4−5 cm); washed with heptane, deionized water, and absolute ethanol; and dried with a stream of dry N_2 gas. Homogeneous (unpatterned) SAMs were prepared by immersing the substrate in a 1.0 mM solution of alkanethiol in anhydrous ethanol. For SAMs terminated by COOH, the alkanethiol was mercaptohexadecanoic acid ($HS(CH_2)_{15}COOH$); for SAMs terminated by CH_3, hexadecanethiol ($HS(CH_2)_{15}CH_3$) was used.

Heterogeneous (patterned) SAMs were prepared by microcontact printing.[9,10] Microcontact printing transfers by contact

(6) Johnson, R. E., Jr.; Dettre, R. H. *J. Phys. Chem.* **1964**, *68*, 1744.
(7) Neumann, A. W.; Good, R. J. *J. Colloid Interface Sci.* **1972**, *38*, 341.
(8) Drelich, J.; Miller, J. D. *J. Colloid Interface Sci.* **1994**, *164*, 252.
(9) Kumar, A.; Whitesides, G. M. *Appl. Phys. Lett.* **1993**, *63*, 2002.
(10) Kumar, A.; Biebuyck, H. A.; Whitesides, G. M. *Langmuir* **1994**, *10*, 1498.
(11) Drelich, J.; Miller, J. D.; Kumar, A.; Whitesides, G. M. *Colloids Surf., A: Physicochem. Eng. Aspects* **1994**, *93*, 1.

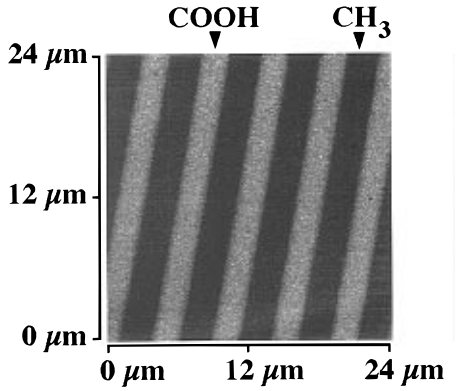

Figure 2. Scanning electron micrograph of a model heterogeneous surface composed of 2.45 μm wide hydrophilic strips (Au−S$(CH_2)_{15}$COOH) and 2.55 μm wide hydrophobic strips (Au−S$(CH_2)_{15}CH_3$).

alkanethiol "ink" from an elastomeric "stamp" to a gold surface: if the stamp is patterned, a patterned SAM forms.[9,10] The stamp is fabricated by casting polydimethylsiloxane (PDMS) on a master having the desired pattern. Masters are prepared using standard photolithographic techniques or are constructed from existing materials having microscale surface features.

For the present experiments, we used an elastomeric stamp, cast from a master produced photolithographically, with an array of 2.5 μm wide lines separated by 2.5 μm wide spaces. Microcontact printing with $HS(CH_2)_{15}CH_3$ formed ~2.55 μm wide lines of SAMs terminated by CH_3, separated by ~2.45 μm wide spaces of bare gold. Exposing the sample (after microcontact printing) to a 1.0 mM solution of $HS(CH_2)_{15}$COOH in anhydrous ethanol formed SAMs terminated by COOH on surface regions of gold not derivatized by the microcontact printing process (the spaces between the lines of SAMs terminated by CH_3). Figure 2 shows an image (by lateral force microscopy[12]) of a 24 μm × 24 μm region of the patterned SAM formed by this process. Light regions of the image correspond to SAMs terminated by COOH.[13] The roughness of the surface results from the crystallinity of 1000 Å thick films of gold prepared by electron-beam evaporation. The fidelity and regularity of the pattern in Figure 2 is typical of the samples used in these experiments. Images similar to Figure 2 were obtained over many regions of a 1 cm^2 sample and were reproducible on different samples.

Imaging of the Patterned Surface. Scanning probe microscopy measurements (AFM, LFM) were performed with a Topometrix TMX 2010 scanning probe microscope (Mountain View). A cantilever fabricated from silicon nitride, in constant contact with the surface, scanned across the substrate at a constant rate (~150 μm/s for a 50 μm region) and with a constant force (~0.1 nN). The patterned SAMs were imaged at room temperature and ambient humidity (40−60%).

Contact Angle Measurements. The sessile-drop technique, which is described in the literature,[14−17] was used in these studies for contact angle measurements using an NRL goniometer (Ramé-Hart, Inc.). The optical system of the NRL goniometer has independently-rotatable cross hairs and an internal protractor readout calibrated in 1° increments. The supporting stage of the instrument is calibrated on both horizontal and vertical axes in 0.02 mm divisions.

The model sample was washed with distilled/deionized water and ethanol, dried, and placed in a controlled-atmosphere Ramé-Hart chamber. The chamber was partially filled with the liquid used for the contact angle measurements to maintain liquid-saturated air. A drop of liquid was placed at the surface of the substrate using a microsyringe. The needle of the syringe remained in contact with the drop and did not distort the spherical shape of the drop. The three-phase contact line of the liquid drop was made to advance or retreat by adding or withdrawing a small volume of liquid. The advancing and receding contact angles were measured at both sides of the drop after about 30−45 s delay. The contact angles were measured with an accuracy of ±1°, for varying drop size.

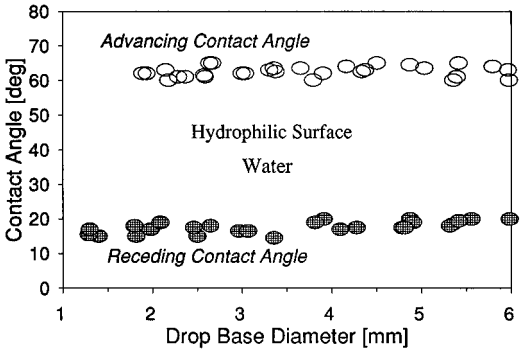

Figure 3. Effect of drop size on advancing and receding contact angle for water drops at the self-assembled monolayer of mercaptohexadecanoic acid (Au−S$(CH_2)_{15}$COOH) as obtained with the sessile-drop technique.

The dynamic captive-bubble technique[8,16−18] was used for the examination of the effect of bubble size on the contact angle. Air bubbles of varying size (diameter = 0.05−3 mm) were generated in the liquid with a syringe under the solid surface. These bubbles were captured at the surface of the substrate as a result of bouyant transport and attachment. A Zeiss stereo-microscope coupled with a camera was used to examine the size of the bubbles at the solid surface. The contact angles were measured from photographs with an accuracy of ±1−2°.

Distilled and deionized water (pH = 5.8 ± 0.1), commercial buffers (pH = 8.0, 10.0, 11.0) freshly prepared, ethylene glycol (99.5%, Mallinckrodt, Inc.), glycerol (99.5%, EM Science), formamide (98%, Mallinckrodt, Inc.), diiodomethane (99%, Aldrich Chemical Co., Inc.), and hexadecane (99%, Aldrich Chemical Co., Inc.) were used in the contact angle experiments. The surface tensions of these liquids were measured with the ring method of de Noüy using a Digital-Tensiometer K10T (KRÜSS, GmbH, Germany), taking into account the correction factors of Harkins and Jordan.

All experiments were performed at 21 ± 1 °C.

Results and Discussion

Wetting Characteristics of Hydrophilic Surfaces. A self-assembled monolayer (SAM) terminated by COOH was used as the "hydrophilic" surface. This SAM was prepared by immersing freshly deposited gold films into a solution of mercaptohexadecanoic acid. Mercaptohexadecanoic acid formed a self-assembled monolayer at the gold surface with a gold−sulfur bond and the carboxylic acid group oriented into the environment.[19,20]

The advancing and receding contact angles for liquid drops (aqueous phase with varying pH, ethylene glycol, glycerol, formamide, and hexadecane) of varying drop base diameter (1−6 mm)[21] were measured with a goniometer using the sessile-drop technique. Figures 3−5 show plots of contact angle vs drop size for drops of distilled water (pH = 5.8 ± 0.2), ethylene glycol, and glycerol on SAMs terminated by COOH (hydrophilic). Similar data il-

(12) For recent reviews of scanning probe microscopy studies on organic surfaces, see: Fuchs, H. *J. Mol. Struct.* **1993**, *292*, 29. Frommer, J. *Angew. Chem., Int. Ed. Engl.* **1992**, *31*, 1265.

(13) Wilbur, J. L.; Biebuyck, H. A.; MacDonald, J. C.; Whitesides, G. M. *Langmuir* **1995**, *11*, 825.

(14) Johnson, R. E., Jr.; Dettre, R. H. *Surf. Colloid Sci.* **1969**, *2*, 85.

(15) Neumann, A. W.; Good, R. J. *Surf. Colloid Sci.* **1979**, *11*, 31.

(16) Drelich, J.; Miller, J. D. *Preprints of the SME Annual Meeting*, Denver, CO, March 6−9, 1995; SME/AIME; Littleton, CO, 1995; Preprint No. 95−11.

(17) Drelich, J.; Miller, J. D.; Good, R. J. *J. Colloid Interface Sci.*, in press.

(18) Drelich, J.; Miller, J. D.; Hupka, J. *J. Colloid Interface Sci.* **1993**, *155*, 379.

(19) Troughton, E. B.; Bain, C. D.; Whitesides, G. M.; Nuzzo, R. G.; Allara, D. L.; Porter, M. D. *Langmuir* **1988**, *4*, 365.

(20) Whitesides, G. M.; Laibinis, P. E. *Langmuir* **1990**, *6*, 87.

(21) The liquid drops with a base diameter less than 1 mm were difficult to place on the substrate surface without any disturbance of drop shape, and thus, the contact angles as measured for such small drops were very uncertain and they are not reported in this contribution.

Table 1. Wetting Characteristics of Hydrophilic Surface, Au−S(CH$_2$)$_{16}$COOH

liquid	pH	surface tension (mN/m)	contact angle[a] θ_A (deg)	θ_R (deg)	$\Delta\theta$ (deg)	line/pseudo-line tension (J/m)
deionized water	5.8	72.4	60−65	15−20	40−50	$-(8.7 \pm 9.4) \times 10^{-9}$
buffer solution	8.0	71.8	58−64	13−18	40−51	$-(7.2 \pm 6.6) \times 10^{-9}$
buffer solution	10.0	71.2	50−55	0	50−55	$-(5.6 \pm 8.9) \times 10^{-9}$ [b]
buffer solution	11.0	71.4	48−52	0	48−52	ND
ethylene glycol		47.8	51−53	18−23	28−35	ND
glycerol		63.4	64−66	<8	56−66	ND
formamide		58.0	55−57	<7	48−57	ND
hexadecane		27.5	<5	0	<5	ND

[a] Contact angles are reported for the drop base diameter from 4 to 6 mm. [b] Uncertain result due to the small number of experimental data; θ_A, θ_R, and $\Delta\theta$ are the advancing contact angle, receding contact angle, and contact angle hysteresis ($\Delta\theta = \theta_A - \theta_R$), respectively; ND = not determined.

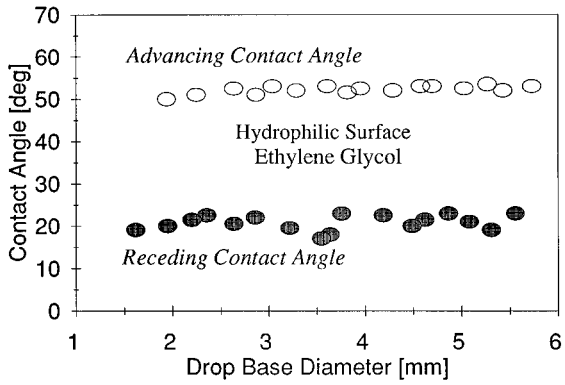

Figure 4. Effect of drop size on advancing and receding contact angle for ethylene glycol drops at the self-assembled monolayer of mercaptohexadecanoic acid (Au−S(CH$_2$)$_{15}$COOH) as obtained with the sessile-drop technique.

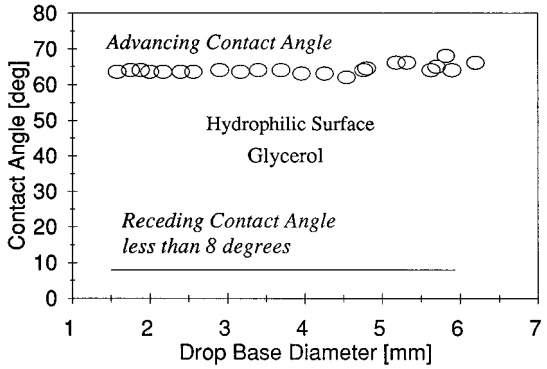

Figure 5. Effect of drop size on advancing and receding contact angle for glycerol drops at the self-assembled monolayer of mercaptohexadecanoic acid (Au−S(CH$_2$)$_{15}$COOH) as obtained with the sessile-drop technique.

lustrating the relationship between contact angle and drop size were also obtained for buffer solutions with varying pH (from pH = 8.0 to pH = 11.0), formamide, and hexadecane. The experimental contact angle data of all liquids studied on a COOH-terminated SAM are reported in Table 1.

In previous studies,[16,17] we found that the variation of contact angle with drop (bubble) size provided useful information about the quality of the surface. We observed that the contact angle hysteresis remained unchanged with varying drop size for close-to-ideal systems, i.e., systems with homogeneous and smooth solid surfaces. Different contact angle/drop size correlations were found for nonideal systems with heterogeneous and/or rough solid surfaces. For these systems, the contact angle hysteresis increased with decreasing drop size.

In the present study, we observed that advancing contact angles remained essentially unchanged (±1−2°) for drop base diameters of 1−6 mm. Similar correlations have been reported for other systems.[16,17] The advancing contact angle, however, is much less sensitive to solid surface imperfections than the receding contact angle. In this regard, the receding contact angle always should receive more attention in the analysis of the surface quality.[16,17] We observed a slight effect of drop size on receding contact angle for some samples in this study, and these experimental data suggest that hydrophilic monolayers deviate from perfect homogeneity and/or cleanness. For example, the receding contact angle decreased by 3−5° with a decrease of drop base diameter from 6 mm to about 1−2 mm for the system with distilled water (Figure 3) and for the system with ethylene glycol (Figure 4). Such changes were not observed for other systems (glycerol (Figure 5) and (not shown here) buffer solutions of pH = 10.0 and 11.0, formamide, and hexadecane) because of zero or close-to-zero receding contact angles for these systems (see Table 1). Also, we observed that the wetting properties of the hydrophilic surface changed with the time of exposure to water. After several experiments with the same sample, the advancing and receding contact angles for distilled water increased from 60−65° and 15−20° to 75−80° and 35−40°, respectively. When the advancing contact angle approached 70° and more, we found that such SAMs terminated by COOH were only slightly sensitive (±3−5°) to variation in pH. Although the SAMs were washed with ethanol and distilled water before measurement and precautions were taken to avoid contamination, adsorption/deposition of contaminants still occurred and affected the contact angle measurements. It should be noted that the liquids used in all the experiments were not the highest purity and that impurities from them could contribute to the contamination of the model SAMs. In this regard, samples which provided "reproducible" contact angle data were used two or three times in the experiments. These selected samples, however, had different wetting characteristics than previously reported for similar substrates. For example, when the wetting properties of SAMs terminated by COOH were tested with distilled water, the advancing and receding contact angles (sessile-drop technique) were found to be 60−65° and 15−20°, respectively (see Table 1). These values are significantly different from those observed in previous measurements:[19] the advancing contact angle for a freshly prepared monolayer of mercaptohexadecanoic acid was found to be less by 10°.

Wetting Characteristics of Hydrophobic Surfaces. SAMs formed from hexadecanethiol on gold were used as model hydrophobic surfaces. The advancing and receding contact angles were measured on these SAMs for liquid drops (aqueous phase with varying pH, ethylene glycol, glycerol, formamide, hexadecane, and diiodomethane) of varying base diameter (1−6 mm). The experimental data for distilled water, ethylene glycol, and glycerol are shown

Table 2. Wetting Characteristics of Hydrophobic Surface, Au−S(CH$_2$)$_{16}$CH$_3$

liquid	pH	surface tension (mN/m)	contact angle[a] θ_A (deg)	θ_R (deg)	$\Delta\theta$ (deg)	line/pseudo-line tension (J/m)
deionized water	5.8	72.4	109−112	96−99	10−16	$-(2.1 \pm 2.8) \times 10^{-8}$
buffer solution	8.0	71.8	108−111	94−96	12−17	$-(4.5 \pm 3.5) \times 10^{-9}$
buffer solution	10.0	71.2	105−109	89−93	12−20	$-(3.1 \pm 11.6) \times 10^{-9}$
buffer solution	11.0	71.4	104−108	86−92	12−22	ND
ethylene glycol		47.8	76−79	48−51	25−31	ND
glycerol		63.4	94−96	73−75	19−23	ND
formamide		58.0	92−94	71−74	18−23	ND
hexadecane		27.5	44−46	32−34	10−13	ND

[a] Contact angles are reported for the drop base diameter from 4 to 6 mm; θ_A, θ_R, and $\Delta\theta$ are the advancing contact angle, receding contact angle, and contact angle hysteresis ($\Delta\theta = \theta_A - \theta_R$), respectively; ND = not determined.

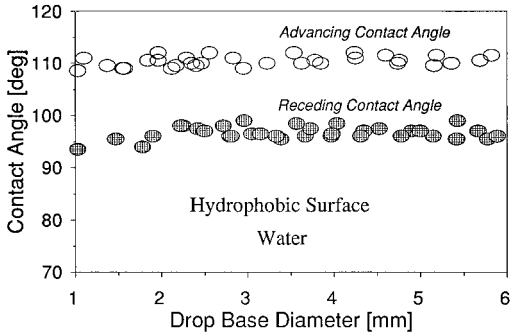

Figure 6. Effect of drop size on advancing and receding contact angle for water drops at the self-assembled monolayer of hexadecanethiol (Au−S(CH$_2$)$_{15}$CH$_3$) as obtained with the sessile-drop technique.

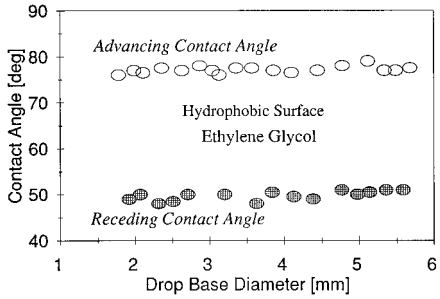

Figure 7. Effect of drop size on advancing and receding contact angle for ethylene glycol drops at the self-assembled monolayer of hexadecanethiol (Au−S(CH$_2$)$_{15}$CH$_3$) as obtained with the sessile-drop technique.

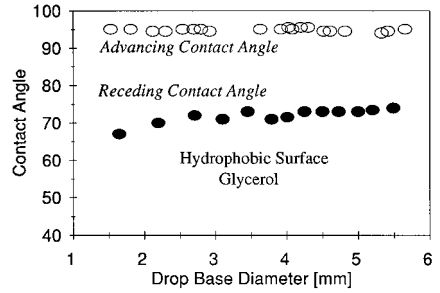

Figure 8. Effect of drop size on advancing and receding contact angle for glycerol drops at the self-assembled monolayer of hexadecanethiol (Au−S(CH$_2$)$_{15}$CH$_3$) as obtained with the sessile-drop technique.

in Figures 6−8. Similar contact angle/drop size measurements were also performed for buffer solutions with varying pH (from pH = 8.0 to pH = 11.0), formamide, and hexadecane. The data for all liquid drops on a hydrophobic surface (base diameter 4−6 mm) are presented in Table 2.

We observed that the values of contact angle for the SAMs terminated by CH$_3$ were in close agreement with

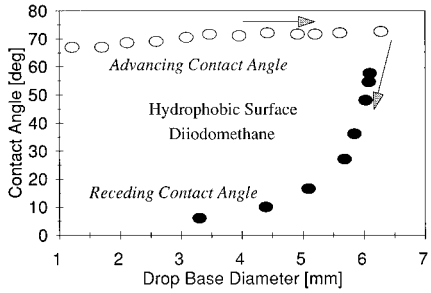

Figure 9. Effect of drop size on advancing and receding contact angle for diiodomethane drops at the self-assembled monolayer of hexadecanethiol (Au−S(CH$_2$)$_{15}$CH$_3$) as obtained with the sessile-drop technique. The arrows indicate the direction of the drop size change.

those reported previously.[19,22] No significant change in the advancing contact angles was found when the drop base diameter was increased from about 1−2 mm to 6 mm (Figures 6−8). The receding contact angle, however, decreased with decreasing drop volume, particularly when the drop base diameter was reduced below 2−3 mm (see Figures 6 and 8). We observed a similar variation of the receding contact angle with varying drop size for heterogeneous, rough, and/or unstable surfaces.[16,17,23] Gold films used in this study were smooth with roughness steps about 5−10 nm (height). In this regard, the surface roughness was not a main reason for the observed changes in contact angle. It is expected that surface contamination occurred to a certain extent and caused the receding contact angle variation. The receding contact angle values, however, were not widely scattered and were reproducible (±1−3°) for a given drop size.

Figure 9 shows the advancing and receding contact angles when measured for diiodomethane drops with varying drop size. The advancing contact angle remained at almost the same level of 70−72° over the range of drop base diameter from 3 mm to 6.5 mm. The receding contact angle decreased with decreasing drop volume (Figure 9). We hypothesize that the SAM was not stable in the presence of diiodomethane. In support of this hypothesis, a similar variation in contact angle occurred with drop size for unstable Langmuir−Blodgett carboxylate films that had been deposited at a calcite crystal surface.[23] Because of the instability of SAMs toward diiodomethane, this liquid was eliminated from further experiments.

Line/Pseudo-line Tensions for Homogeneous Monolayers. The relationship between contact angle and bubble size was examined with the dynamic captive-bubble technique. Air bubbles of varying volume were generated

(22) Bain, C. D.; Troughton, E. B.; Tao, Y-T.; Evall, J.; Whitesides, G. M.; Nuzzo, R. G. *J. Am. Chem. Soc.* **1989**, *111*, 321.

(23) Jang, W.-H.; Drelich, J.; Miller, J. D. *Preprints of the SME Annual Meeting*, Denver, CO, March 6−9, 1995; SME/AIME: Littleton, CO, 1995; Preprint No. 95−96. Jang, W.-H.; Drelich, J.; Miller, J. D. *Langmuir* **1995**, *11*, 3491.

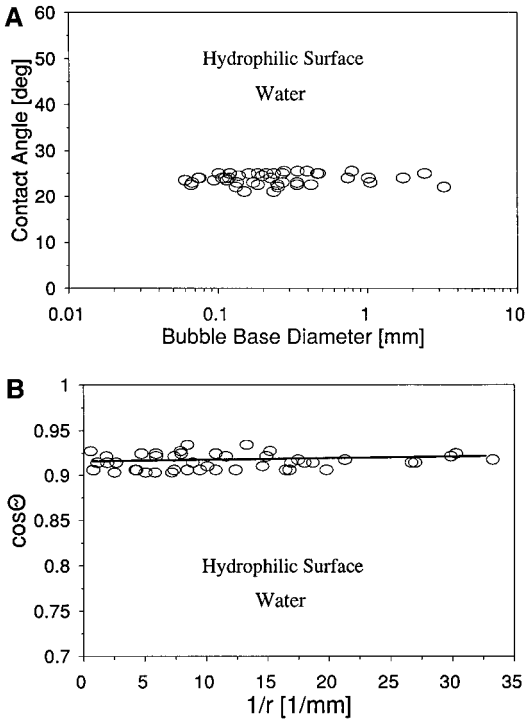

Figure 10. Effect of bubble size on contact angle for the air/water/(Au−S(CH$_2$)$_{15}$COOH) system as obtained with the dynamic captive-bubble technique: (A) contact angle vs bubble base diameter; (B) cosine of the contact angle vs reciprocal of the bubble base radius.

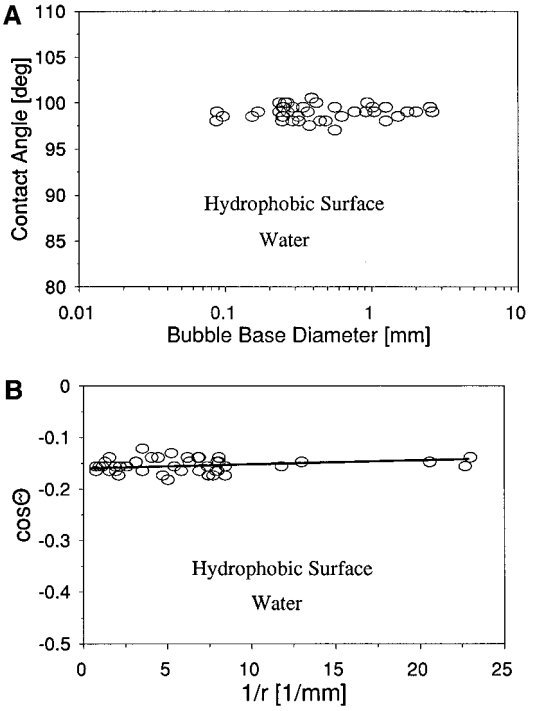

Figure 11. Effect of bubble size on contact angle for the air/water/(Au−S(CH$_2$)$_{15}$CH$_3$) system as obtained with the dynamic captive-bubble technique: (A) contact angle vs bubble base diameter; (B) cosine of the contact angle vs reciprocal of the bubble base radius.

in the bulk liquid beneath the hydrophobic or hydrophilic surface with a syringe and allowed to be captured at the surface. Photographs of air bubbles attached to the model surface were taken, and the contact angles and bubble dimensions were measured from these photographs. An advantage of this technique is the ability to examine the relationship between contact angle and bubble size for bubbles ranging from several micrometers to several millimeters in diameter. The line/pseudo-line tension[24] values can also be determined from the cos θ vs $1/r$ relationship (θ is the contact angle; r is the bubble base radius), according to the modified Young's equation (eq 3).

Figures 10 and 11 present the contact angle values as measured for distilled water at the hydrophilic and hydrophobic surfaces, respectively, for varying bubble size. Similar contact angle/bubble size relationships were obtained for buffer solutions of pH = 8.0 and 10.0 (only a few air bubbles were able to attach at the hydrophilic surface in the buffer solution of pH = 10.0, and thus, the experimental data for this system were limited). Other systems were not examined in this study due to difficulties with deposition of gas bubbles at the SAMs in the environment of such liquids as the buffer solution with pH = 11.0, ethylene glycol, glycerol, formamide, and hexadecane.

The contact angles as determined with the dynamic captive-bubble technique corresponded to the receding and intermediate (between advancing and receding) contact angles as measured with the sessile-drop technique[16,17] (Table 1). A 2−5° scatter in contact angle values was observed. In other studies, much larger scatter in the contact angle data was reported for the dynamic captive-bubble technique when rough and/or heterogeneous surfaces were examined.[8,18] Thus, these data also indicate that the SAMs were well prepared with regard to smoothness of the substrate and homogeneity of the surface. However, as discussed in the previous paragraphs, some surface defects/contamination affected the contact angle measurements to a certain extent.

The contact angles decreased with decreasing bubble volume for all systems. The relationship between contact angle and bubble size for distilled water at the hydrophilic and hydrophobic surfaces is presented in Figures 10B and 11B. The linear correlation between the cosine of the contact angle (cos θ) and the reciprocal of the bubble base radius ($1/r$) was obtained, and this linearity satisfies the modified Young's equation (eq 3). Equation 3 predicts that the line tension can be calculated from the slope of the line plotting cos θ vs $1/r$, for an ideal three-phase system involving a pure liquid and a homogeneous, smooth, isotropic, and rigid solid surface. Unfortunately, the surfaces examined were not ideal. The contact angle hysteresis was always significant for the surfaces being examined (see Tables 1 and 2), and a 2−3° scatter in contact angle values was observed during measurement of the advancing and receding contact angle (sessile-drop technique). A precaution must therefore be taken in the interpretation of the correlation between contact angle and bubble size (Figures 10 and 11) because the relationship between contact angle and bubble size may not be simply affected by the line tension alone as expected from the modified Young's equation (eq 3). For such systems, the term "pseudo-line tension" is recommended to describe the value calculated from the cos θ vs $1/r$ correlation in order to distinguish the experimental observation from the actual thermodynamic line tension.[18,25]

The line/pseudo-line tension values were determined for systems with distilled water and buffer solutions of pH = 8.0 and 10.0, and they are presented in Tables 1 and

(24) Line tension: the excess free energy of the system at the three-phase contact line. The line/pseudo-line tension term is used in this paper to describe the value calculated from the cos θ vs $1/r$ function. At the present time, we are not able to discuss how close our experimentally-measured pseudo-line tensions are to the actual thermodynamic line tensions.

(25) Good, R. J.; Koo, M. N. *J. Colloid Interface Sci.* **1979**, *71*, 283.

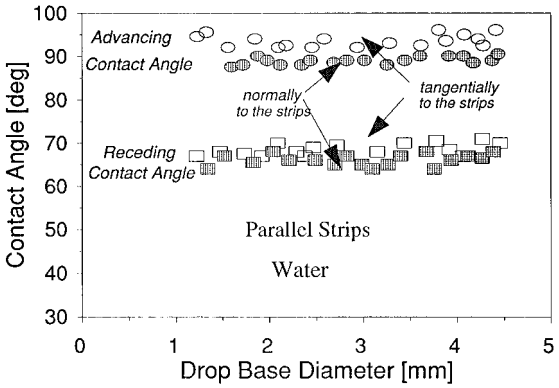

Figure 12. Effect of drop size on advancing and receding contact angle for water drops at a model heterogeneous surface consisting of 2.45 μm wide strips of self-assembled monolayer terminated by COOH (Au−S$(CH_2)_{15}$COOH) and 2.55 μm wide strips of self-assembled monolayer terminated by CH_3 (Au−S$(CH_2)_{15}CH_3$).

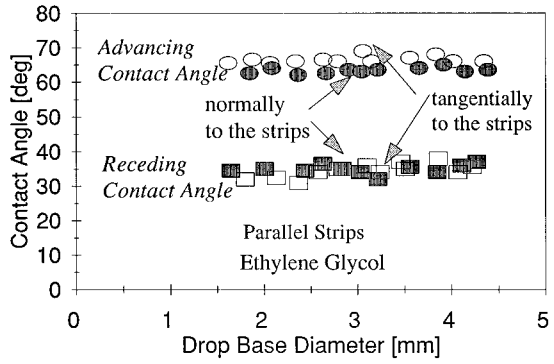

Figure 13. Effect of drop size on advancing and receding contact angle for ethylene glycol drops at a model heterogeneous surface consisting of 2.45 μm wide strips of self-assembled monolayer terminated by COOH (Au−S$(CH_2)_{15}$COOH) and 2.55 μm wide strips of self-assembled monolayer terminated by CH_3 (Au−S$(CH_2)_{15}CH_3$).

2. The hydrophilic surface had the line tension value -5.6×10^{-9} J/m to -8.7×10^{-9} J/m (Table 1), and the hydrophobic surface had -3.1×10^{-9} J/m to -2.1×10^{-8} J/m (Table 2). The 2−5° scatter in contact angle values and the narrow range of bubble size examined (0.04−2 mm diameter base) affect the accuracy of the line/pseudo-line tension values. As presented in Tables 1 and 2, the confidence intervals for the line/pseudo-line tension values determined are of the same order of magnitude as the average values. In this regard, the line/pseudo-line tension values remain uncertain.

Finally, it needs to be emphasized that the hydrophobic and hydrophilic surfaces prepared and examined in this study were found to be of higher quality than those examined in previous studies (surfaces were certainly less contaminated and/or monolayers better organized).[11] The line/pseudo-line tension values obtained in this study (Tables 1 and 2) were found to be one or two orders of magnitude smaller than those reported in the previous contribution,[11] and these values are very close to those values which are expected for perfect homogeneous surfaces (from 10^{-12} to 10^{-9}−10^{-8} J/m).[8]

Wetting Characteristics of Liquid Drops at Model Heterogeneous Surfaces. Heterogeneous surfaces consisting of alternating and parallel 2.55 μm hydrophobic (Au−S$(CH_2)_{16}CH_3$) and 2.45 μm hydrophilic (Au−S$(CH_2)_{16}$COOH) strips were prepared on a gold surface (a 2000 Å gold film supported on a Si/SiO_2/Ti substrate) by patterning self-assembled monolayers, using an elastomer stamp.[9,10] The wetting characteristics of these model

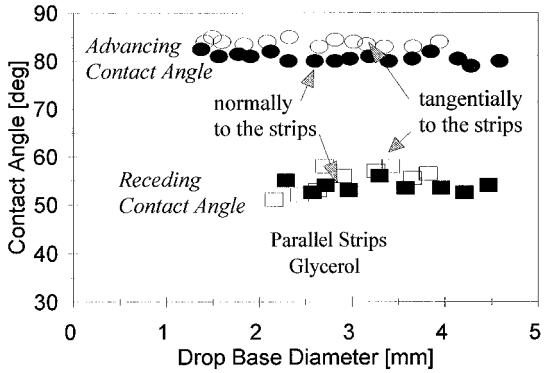

Figure 14. Effect of drop size on advancing and receding contact angle for glycerol drops at a model heterogeneous surface consisting of 2.45 μm wide strips of self-assembled monolayer terminated by COOH (Au−S$(CH_2)_{15}$COOH) and 2.55 μm wide strips of self-assembled monolayer terminated by CH_3 (Au−S$(CH_2)_{15}CH_3$).

heterogeneous surfaces were examined by contact angle measurements using the sessile-drop technique. The advancing and receding contact angles for liquid drops (distilled water, buffer solutions of pH = 8.0, 10.0, and 11.0, ethylene glycol, ethylene glycol, glycerol, formamide, and hexadecane) were measured with the strips both parallel to and normal to the three-phase contact line. Figures 12−14 illustrate examples of contact angle results obtained for this model heterogeneous surface with liquid (water, ethylene glycol, and glycerol) drops of varying size. Similar contact angle/drop size relationships were obtained for buffer solutions, formamide, and hexadecane. The advancing and receding contact angle data for all liquids are presented in Table 3.

The relationship between the contact angle and the drop size was linear for both advancing and receding contact angles when the drop base diameter was decreased from about 5 to 2 mm. A 2−4° scatter in contact angle was commonly observed (Figures 12−14). In some experiments, the contact angle—especially the receding contact angle—significantly decreased with decreasing drop size. If this behavior was observed, the heterogeneous surface was replaced, assuming that the nonlinear correlation between contact angle and drop size was caused by surface contaminants (deposited dust particles and adsorbed organic compounds from the laboratory environment are the most common and undesirable contaminants).

The advancing and receding contact angles measured with the drop edge normal to the strips were found to be 2−10° lower (Table 3) than those measured with the drop edge parallel to the strips (Figure 1). The effect of contortion of the three-phase contact line on contact angle is evident. Even a stronger effect of the wetting line contortion on the advancing contact angle (8−16° difference between contact angles as measured at contorted and noncontorted water drop edge) was reported in our previous contribution;[11] however, heterogeneous surfaces with different strip dimensions and different wetting characteristics were used in the previous studies.

A 2−4° scatter in contact angle values was commonly observed during measurements, particularly during receding contact angle measurements. This variation in the value of the contact angle was more pronounced for liquid drop edges situated parallel to the strips. Also, different contact angles, smaller and larger, than those presented in Table 3 were sometimes observed for such position of the three-phase contact line at parallel strips. These results may suggest that the system could adopt metastable configurations with a different apparent contact angle. On the other hand, surface defects or

Table 3. Wetting Characteristics of the Model Heterogeneous Surface Composed of Alternating and Parallel 2.45 μm Hydrophilic, Au−S(CH$_2$)$_{16}$COOH, and 2.55 μm Hydrophobic, Au−S(CH$_2$)$_{16}$CH$_3$, strips

			contact angle[a]					
			measured tangential to the strips			measured normal to the strips		
liquid	pH	surface tension (mN/m)	θ_A (deg)	θ_R (deg)	$\Delta\theta$ (deg)	θ_A (deg)	θ_R (deg)	$\Delta\theta$ (deg)
deionized water[b]	5.8	72.4	92−96	67−71	21−29	88−90	65−68	20−25
			89−93	64−69	20−29	84−89	62−66	18−27
buffer solution[b]	8.0	71.8	90−94	65−68	22−29	84−88	60−64	20−28
			87−92	64−67	20−28	83−86	61−65	18−25
buffer solution[b]	10.0	71.2	80−85	43−47	33−42	74−79	36−40	34−43
			79−83	48−52	27−35	70−76	40−43	27−36
buffer solution	11.0	71.4	76−80	20−25	51−60	71−76	38−42	29−38
ethylene glycol		47.8	66−69	34−38	28−35	62−65	32−37	25−33
glycerol		63.4	84−86	55−58	26−31	79−82	54−56	23−28
formamide		58.0	75−78	45−49	26−33	65−68	44−46	19−24
hexadecane		27.5	17−21	<5	12−21	12−16	0	12−16

[a] Contact angles are reported for liquid drops with a base diameter from 3 to 5 mm. [b] For these systems the contact angle measurements were repeated for a second set of heterogeneous surfaces; θ_A, θ_R, and $\Delta\theta$ are the advancing contact angle, receding contact angle, and contact angle hysteresis ($\Delta\theta = \theta_A - \theta_R$), respectively. For distilled water and buffer solutions of pH = 8.0 and 10.0, the contact angle measurements were repeated for two sets of model heterogeneous surfaces.

Table 4. Contact Angle Values (θ^C) As Calculated from the Cassie Equation (Eq 1) Using Contact Angle Data for Hydrophilic (Table 1) and Hydrophobic (Table 2) Surfaces and As Determined Experimentally for Model (Parallel Strips) Heterogeneous Surfaces (the Three-Phase Contact Line Is Parallel to the Strips; Noncontorted)

	advancing contact angle θ^C_A (deg)		receding contact angle θ^C_R (deg)	
liquid (pH)	exp	calc	exp	calc
deionized water (5.8)	92−96	85−89	67−71	65−68
	89−93	85−89	64−69	65−68
buffer solution (8.0)	90−94	84−88	65−68	64−66
	87−92	84−88	64−67	64−66
buffer solution (10.0)	80−85	79−83	43−47	60−63
	79−83	79−83	48−52	60−63
buffer solution (11.0)	76−80	78−82	20−25	58−62
ethylene glycol	66−69	64−67	34−38	36−39
glycerol	84−86	80−82	54−57	50−52
formamide	75−78	75−77	45−49	49−51
hexadecane	17−21	31−33	<5	23−24

contaminants could stimulate these differences in contact angle values as well.

Experimental Verification of the Cassie Equation. The contact angles (advancing and receding) measured for the model heterogeneous surface composed of alternating and parallel strips with the three-phase contact line parallel to the strips (Figure 1; no contortion of the three-phase contact line) can be fit by the Cassie equation (eq 1). Here, the subscripts 1 and 2 correspond to the hydrophilic (COOH) and hydrophobic (CH_3) strips, respectively. Using the known (Figure 2) dimensions of the strips, the fractional area of the hydrophilic and hydrophobic regions was calculated to be $f_1 = 0.49$ and $f_2 = 0.51$. On the basis of the data for homogeneous surfaces (from Tables 1 and 2 the smallest and largest values for contact angles were selected for calculation), the advancing and receding contact angles for the heterogeneous surface were calculated from the Cassie equation (eq 1). The results of these calculation are presented in Table 4. Good agreement was obtained between experimental contact angle values, both advancing and receding contact angles, measured at a position where the three-phase contact line was not affected by heterogeneous strips, and those calculated from the theoretical relationship (eq 1) for most of the systems. A significant difference between the values of the receding contact angles and those calculated from the Cassie equation was found for buffer solutions with pH = 10.0 and 11.0 and hexadecane (Table 4). Strong interactions between these liquids and the hydrophilic strips (receding contact angle = 0, Table 1) might be responsible for preferential metastable configurations of the three-phase system which are far away from the equilibrium state (pinning effect). No correlation of experimental and calculated advancing contact angles was observed when the model surface was probed with hexadecane (zero contact angle at the hydrophilic surface, Table 1). Again, this discrepancy indicates that theory may fail for heterogeneous surfaces with patches having a strong affinity for the testing liquid (contact angle = 0).

Experimental Verification of the Modified Cassie Equation. When the edge of the drop was perpendicular to the strips, a contortion of the three-phase contact line was observed. The contortion of the wetting line significantly affected the contact angle value (see experimental data in Table 3). The advancing and receding contact angles for the contorted drop side were 2−10° lower than those for the noncontorted side of the liquid drop and lower than those calculated from the Cassie equation. When the three-phase contact line is contorted, the contact angle should be predicted by the modified Cassie equation (eq 2). For this system, the modified Cassie equation, which incorporates the line/pseudo-line tension term, is as follows

$$\cos\theta^{MC} = f_1\cos\theta_1 + f_2\cos\theta_2 - \left(\frac{1}{\gamma_{LV}}\right)\left(\frac{f_1\gamma_{SLV_1}}{r_1} + \frac{f_2\gamma_{SLV_2}}{r_2}\right) \quad (2a)$$

γ_{SLV} is the line/pseudo-line tension; γ_{LV} is the surface tension of the liquid; and r_1 and r_2 are the half widths of the hydrophilic and hydrophobic strips, respectively. For simplification, we assumed that the contortions of the three-phase contact line at the hydrophilic and hydrophobic strips were symmetrical and that the local deformations of the three-phase contact line affected by these strips were circular with a diameter equal to the width of the strips. These assumptions allow the calculation of the contact angle for the liquid drop with a contorted three-phase contact line; they are, however, rough approximations. Although the shape of the drop edge may be more complex, microscopic observations of the corrugated three-phase contact line indicated that the shape of the wetting line was close to the assumed shape. Accurate radii of the local deformations, however, could not be determined due to the limited magnification of the optical stereoscopic microscope used in this study (Figure 15).

The advancing and receding contact angle values for heterogeneous surfaces, where the drop edge is situated

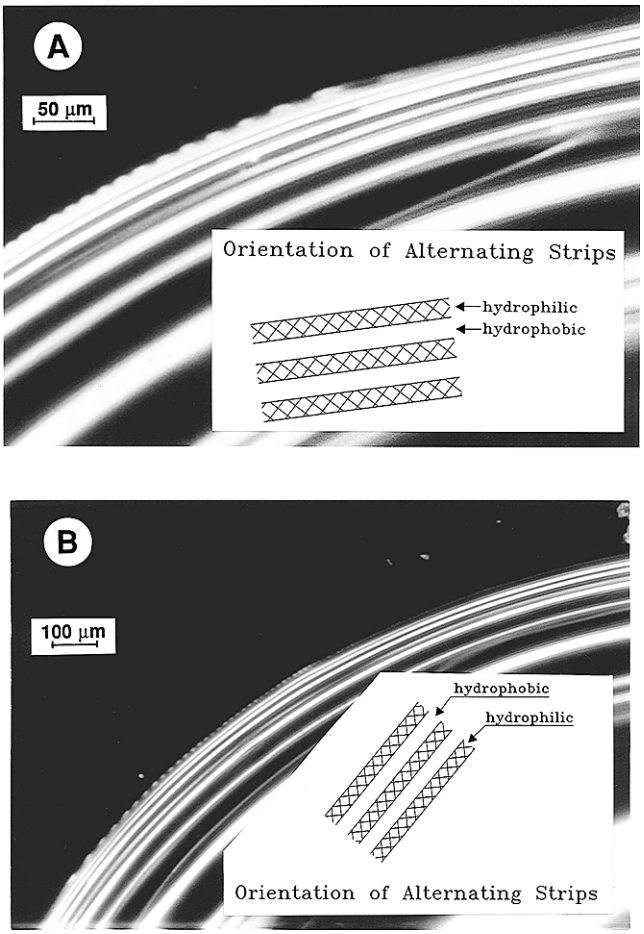

Figure 15. Contortion of the three-phase contact line as observed by optical microscopy for a drop of water (A) and glycol (B) located at the model heterogeneous surface consisting of alternating and parallel 2.55 μm hydrophobic and 2.45 μm hydrophilic strips. The drop edge is observed from above. The orientation of alternating and parallel strips is illustrated as a point of reference. It appears quite clearly from these photographs that hydrophobic and hydrophilic strips exhibit different wetting properties and that a different local contact angle exists at each strip. Consequently, the three-phase contact line is contorted. Unfortunately, the exact shape of the contact line cannot be well defined from these photographs due to limited magnification of the images which were obtained with a stereoscopic microscope.

normal to the strips, were also calculated using the modified Cassie equation (eq 2a) (Table 5). The advancing and receding contact angles as determined for fully hydrophilic and hydrophobic surfaces (from Tables 1 and 2 the smallest and largest contact angles were selected for calculations), and line/pseudo-line tension values taken from Tables 1 and 2 (average values) were used in these calculations. Additional calculations were performed for systems assuming selected values for the line/pseudo-line tension of -1×10^{-9} J/m and -1×10^{-8} J/m.[26]

There is good agreement between the experimental contact angles and those calculated for most of the systems when the line/pseudo-line tension values from Tables 1 and 2 or the theoretical values of -1×10^{-9} J/m and -1×10^{-8} J/m were used in the calculations (Table 5). Again no agreement was obtained for buffer solutions of pH = 10.0 and 11.0. For these systems, the experimental receding contact angles were found to be 10−20° smaller than the theoretical values (Table 5). A strong interaction between the buffer solutions and the hydrophilic strips (receding contact angles = 0, Table 1) could cause unpredictable behavior of the wetting line at a heterogeneous surface.

(26) This assumption with regard to the order of magnitude seems to be reasonable in view of the experimental data obtained for a few systems, see Tables 1 and 2.

Table 5. Advancing and Receding Contact Angles As Determined Experimentally for Model (Parallel Strips) Heterogeneous Surfaces (the Three-Phase Contact Line Is Normal to the Strips; Contorted) and Contact Angle Values (θ^{MC}) As Calculated from the Modified Cassie Equation Using Contact Angle Data for Hydrophilic (Table 1) and Hydrophobic (Table 2) Surfaces and Using the Line/Pseudoline Tensions from Tables 1 and 2 and Assuming Values of $\gamma_{SLV_1} = \gamma_{SLV_2} = -1 \times 10^{-8}$ J/m and -1×10^{-9} J/m

	advancing contact angle θ^{MC}_A (deg)		receding contact angle θ^{MC}_R (deg)	
liquid (pH)	exp	calc	exp	calc
deionized water (5.8)	84−90	80−84[a]	62−68	61−64[a]
		83−87[b]		64−67[b]
		89−93[c]		70−73[c]
buffer solution (8.0)	83−88	85−89[a]	60−65	66−67[a]
		82−86[b]		63−65[b]
		88−92[c]		69−71[c]
buffer solution (10.0)	70−79	81−85[a]	36−43	63−65[a]
		78−82[b]		58−61[b]
		84−87[c]		65−68[c]
buffer solution (11.0)	71−76	72−75[b]	38−42	50−54[b]
		78−81[c]		58−61[c]
ethylene glycol	62−65	56−58[b]	32−37	18−24[b]
		66−68[c]		37−40[c]
glycerol	79−82	72−74[b]	55−58	40−42[b]
		79−81[c]		49−51[c]
formamide	65−68	66−68[b]	44−46	37−40[b]
		74−76[c]		48−50[c]
hexadecane	12−16	0[b]	0	0[b]
		28−29[c]		18−20[c]

[a] Values found using the line/pseudo-line tensions from Tables 1 and 2. [b] Values found assuming $\gamma_{SLV_1} = \gamma_{SLV_2} = -1 \times 10^{-8}$ J/m. [c] Values found assuming $\gamma_{SLV_1} = \gamma_{SLV_2} = -1 \times 10^{-9}$ J/m.

The contact angles for all organic liquids were calculated on the basis of theoretically assumed line/pseudo-line tension values, -1×10^{-9} J/m and -1×10^{-8} J/m. The data in Table 5 indicate good agreement between experimental and calculated contact angle values when such order of magnitude of line/pseudo-line tension values were selected.

Summary and Conclusions

Heterogeneous surfaces consisting of alternating and parallel 2.55 μm hydrophobic and 2.45 μm hydrophilic strips were prepared on a gold surface by patterning self-assembled monolayers with an elastomer stamp. Hexadecanethiol and mercaptohexadecanoic acid were used for the formation of model organic monolayers with hydrophobic and hydrophilic properties, respectively. The wetting characteristics of these model heterogeneous surfaces were examined by contact angle measurements with the sessile-drop technique using distilled water, buffer solutions of pH = 8.0, 10.0, and 11.0, ethylene glycol, glycerol, formamide, and hexadecane. For diiodomethane the value of the contact angle was not stable. We hypothesize that diiodomethane damaged the SAM.

The advancing and receding contact angles, when measured with the drop edge normal to the strips (the three-phase contact line was contorted), were found to be ~2−10° lower than those measured with the drop edge parallel to the strips (the three-phase contact line was smooth). These data prove that the micron-size contortion of the three-phase contact line affects the contact angle.

Homogeneous surfaces of SAMs (terminated by CH_3, hydrophobic, and COOH, hydrophilic) were prepared. The

wetting characteristics of these model surfaces were examined with contact angle measurements using the sessile-drop and dynamic captive-bubble techniques. The line/pseudo-line tensions (calculated from the contact angle/bubble size relationship) were -1×10^{-9} to -1×10^{-8} J/m for both hydrophobic and hydrophilic surfaces.

The values of the advancing contact angles, receding contact angles, and line/pseudo-line tension, which were determined for the homogeneous surfaces, were used for theoretical calculations of contact angles for the heterogeneous surfaces consisting of alternating and parallel 2.45 μm hydrophilic and 2.55 μm hydrophobic strips. The theoretical values (as calculated from the Cassie equation and from the modified Cassie equation) were compared with experimental contact angle values. For most systems the experimental advancing and receding contact angles were in good agreement with these theoretical values when the three-phase contact line was noncontorted, i.e., the three-phase contact line was situated along the strip. There was also good agreement between experimental advancing and receding contact angles for the liquid drop edge normal to the strips (the contorted three-phase contact line) and theoretical contact angle values calculated from the modified Cassie equation (which incorporates a contribution of the line/pseudo-line tension to the three-phase system).

No agreement between experimental and theoretical contact angle values was obtained when the liquid demonstrated a strong affinity for the hydrophilic strips (contact angle = 0). These experimental data indicate that the theory expressed by the Cassie equation or modified Cassie equation may fail for heterogeneous surfaces with high-energy surface components.

Acknowledgment. This work was financially supported in part by the National Science Foundation, Grant No. CTS-9215421. J.L.W. gratefully acknowledges a postdoctoral fellowship from the NIH.

LA9509763